Multi-energy microgrid optimal operation with integrated power to gas technology considering uncertainties

Abstract: Multi-Energy Microgrids (MEMGs) have emerged as an invaluable framework for the integration of renewable sources and storage facilities. The operation of such kinds of systems is a challenging task because of the unpredictable nature of renewable sources and demand. In this sense, robust scheduling tools are essential for the proper energy management of MEMGs. This paper deals with the optimal operation of a MEMG, which comprises electric, gas, hydrogen and thermal subsystems. The studied system encompasses various storage technologies, combined heat and power (CHP) units, gas boilers, PV generators, natural gas fuel cells (FCs), micro turbine generator (MTG) and power to gas (P2G) chain for fuel cell electric vehicles (FCEVs) refueling. To manage uncertainties in generation and demand, a bi-stochastic-robust paradigm is proposed, by which the different uncertainties involved are treated by different methods. Thus, information gap decision theory (IGDT) is employed to model electrical and heat loads, while the Hong 2m+1 approach is used to manage the uncertainty of the photovoltaic (PV) system. Moreover, a stochastic approach is applied to cope with the random behavior of FCEVs. The results of the proposed hybrid optimization confirm that various uncertain modelling is appropriate for each stochastic parameter, and combining different approaches in a holistic way can achieve an efficient but reliable methodology.

Index Terms: Microgrid optimal operation; P2G technology; CHP, Heat load, PV array, Fuel cell electric vehicles, IGDT approach, 2m+1 Hong’s approach

Nomenclature

Indexes (sets)

$t(T)$ Time

Superscripts

$buy/sell$	Electrical energy bought/sold from/to the upscale network
$FCEV$	Fuel cell electric vehicle
(700)	Makes mention to the hydrogen compressed at 700 bar
$Comp$	Hydrogen compressor
in/out	Inflow/outflow
$P2G$	Power-to-gas
FC	Fuel cell
MT	Microturbine
CHP	Combined heat and power
$Boil$	Boiler
PV	Photovoltaic units
$BS, ch/dch$	Battery storage in charging/discharging process
LD	Local demand
HS	Hydrogen storage
$\overline{(*)}/\underline{(*)}$	Maximum/minimum value of a variable or parameter

Parameters

$\Delta\tau$	Time step (hrs)
λ	Energy cost ($/kWh)
γ	Compressed hydrogen cost ($/kg)

ρ Hydrogen density (kg/m³)

μ Operation and maintenance costs ($/kWh)

ν Natural gas price ($/m³)

σ Start-up and shutdown costs ($)

υ Nominal gas consumption (m³/kWh)

ε Nominal energy consumption (kWh/m³)

η Efficiency (pu)

Z Compressibility factor

LHV Lower heating value of natural gas (MMBTU/kWh)

h Heat demand (kW)

$\bar{G}^{grid}$ Maximum gas that can be purchased from the network (MMBTU)

R Ramp rate limit (kW)

ϑ Solar irradiation (kW/m²)

θ Temperature (ºC)

$e2P$ Energy-to-power ratio (hrs)

DOD Depth of discharge (pu)

$\bar{q}^{HS}$ Rate flow of the hydrogen storage (m³/h)

Variables

p Power (kW)

g Hydrogen volume (m³)

u Commitment status (binary)

on/off On/off status of assets (binary)

s Energy stored (kWh)

1 - Introduction

A Microgrid (MG) is intended as a small-scale power grid, which encompasses onsite generation units, storage banks and controllable loads, which can work either in islanded or connected modes [1-3]. Nowadays, this concept has attracted great attention with the development of communication infrastructures, control schemes and protection philosophies [4, 5]. As observed in larger systems in the early 21st century [6], the MG paradigm has evolved towards considering multiple energy vectors on a whole. Thus, many research efforts have been recently made on further investigating and modelling multi-energy MGs (MEMGs) [7, 8], as a valuable framework for integrating and jointly managing different energy carriers such as electricity, hydrogen or natural gas. This evolution has been enabled by the maturity of different conversion technologies such as electrolyzers, Combined heat and power (CHP) units, fuel-cells, gas turbines or Power-to-Gas chains [8, 9].

Efficient management of MEMGs can be only achieved by taking economic, technical and environmental concerns into consideration. Nowadays, such issues are usually addressed by means of energy management tools [8]. Conventionally, an energy management program performs a day-ahead optimization of the scheduling plan for the different available assets, ensuring the demand supplying at minimum cost while certain security and technical constraints are satisfied. This issue has been profusely investigated recently considering multiple objectives such as reduction of carbon emissions [10], integration of demand response programs [11], the inclusion of electric and gas vehicles [8], among others. Different mathematical formulations of the energy management problem for MEMGs have been stated from simple linear and Mixed Integer Linear (MIL) formulations [8, 11], to more complex nonlinear problems that are customary, solved using metaheuristic techniques [10]. Nevertheless, MIL formulations are widely preferred because its modularity, simplicity and ability to achieve the global optimum [12].

One main concern in energy management problems for MEMGs is the consideration of uncertainties. Such issue is of great importance because of the high penetration of renewable-based intermittent sources besides low-aggregated loads at MG level [13]. This fact provokes that the scheduling result calculated by energy management problems is subjected to uncertainties that should be properly addressed and quantified. Customarily, uncertainties modelling can be addressed from two points of view. On the one hand, stochastic programming could be performed generating a large number of scenarios based on historical data or well-known probability models. On the other hand, a well-established robust optimization framework could be considered to manage the uncertainty and performs a robust scheduling plan.

Various references have studied energy management in MEMGs through stochastic programming. This approach consists of generating a large number of scenarios (about 1,000 [14]) for the uncertain variables. Then, the scheduling plan for the MG is determined to optimize the objective function over the scenario space instead of considering a unique-scenario approach. This way, one takes into account the randomness of the stochastic parameters. The scenarios can be generated either on the basis of forecast profiles [15], historical data [16] or well-known distribution functions [17]. This methodology is quite simple, however, it normally entails a high computational burden because of the need of evaluating a huge amount of scenarios. Owing to simplicity, stochastic programming has been widely used for energy management tools in MEMGs. One notorious example is the reference [15], in which the authors proposed a stochastic approach for MGs which encompasses hydrogen storage, batteries and renewable sources. In this reference, the scenarios are generated on the basis of forecasted profiles for weather parameters, assuming Gaussian distribution of errors. Similarly, in [17] the real-time energy management of a MEMG with hydrogen and electrical sub-networks is performed by using distribution functions, model predictive control and statistical analysis. In [18] a fuel cell and associated storage are used as a buffer to handle with intermittent behavior of renewable units under a stochastic programming paradigm.

In contrast, robust optimization adopts a single-scenario approach. However, this kind of method manages uncertainty in a conservative manner, frequently considering the most unfavorable values of the uncertain parameters. Normally, this kind of approach allows fixing a level of risk [19], by which the users may set the degree in which variability of uncertain parameters are considered. Thus, if the scheduling plan is performed from a conservative point of view, the random parameters are considered to take high volatility, contrarily, the region of the variability of uncertain parameters becomes narrower at the level of risk decreases until its minimum, which typically corresponds with a deterministic approach. One example of a robust technique is the information gap decision theory (IGDT), which has been used for energy management or economic dispatch of MEMGs in [19, 20]. Other problems raise a min-max optimization problem by which the objective function is minimized while the uncertain set is maximized. The problem can be converted into an only minimization problem by using the duality theorem, however, in this case, the number of variables dramatically grows. The references [21, 22] have exploited this approach for either planning or operation of MEMGs. Some methodologies have used interval optimization [23], by which the problem is used interval arithmetic over a range in which is known that a forecast parameter may lie. This way, the objective function is minimized for the worst predicted case. Finally, the uncertainty can be modelled as extra costs in the objective by means of cost value at risk functions [24]. Thereby, the risk that the MG operator assumes is quantified in the objective as a monetary expenditure.

This paper contributes to uncertain modelling in MEMGs by developing a stochastic-bi-robust optimization framework in which two different robust approaches are combined with the stochastic paradigm in an original way. On the one hand, IGDT is used to model electrical and heat demand, while the Hong 2m+1 approach serves to manage the uncertainty of renewable generation. On the other hand, a stochastic approach is adopted to handle with random behavior of fuel cell electric vehicles (FCEVs) refueling events. The developed hybrid optimization is founded on the fact that different uncertain modelling is suitable for each stochastic parameter, and combining different approaches in a holistic way one can obtain an efficient but reliable methodology. The new proposal is validated in MEMGs which encompasses electrical, gas, heat and hydrogen subnetworks.

The rest of the paper is organized as follows. MEMG description is given in Section 2. Mathematical modelling is presented in Section 3. The developed framework for considering multiple uncertainties is explained in Section 4. Section 5 presents various numerical results on a case study to validate the developed approach. Finally, this paper is concluded with Section 6.

2 - MEMG description

A schematic diagram of the MEMG under study is shown in Fig. 1. Three different energy vectors are encompassed. Firstly, electricity can be purchased from the upscale grid or generated by means of onsite generators such as photovoltaic (PV) arrays, CHP system, Fuel Cell system that fueled directly from Natural Gas (NG) [25,26], and Micro Turbine Generator (MTG). The energy acquisition from the upscale grid has a cost which is imposed by the grid operator by means of a flat or dynamic pricing mechanism. The electricity sub-system also includes a battery storage facility which enables a more efficient management of electric energy [27]. Secondly, NG can be directly acquired from the NG distribution network and injected into a MTG or natural gas fuel cell (NGFC) system to produce electricity, to combined heat and power (CHP) device to produce heat and electricity, or in a boiler to only produce heat. The CHP and boiler facilities jointly supply a local heat load. Finally, gaseous hydrogen can be produced from water electrolysis. This gas is directly compressed at high pressure and stored in tanks, which can supply a local refueling station for fuel-cell hydrogen electric vehicles (FCEVs). Nowadays, FCEVs work in a range of 350-700 bar [28]. In this work for simplicity, we have only considered a 700 bar system.

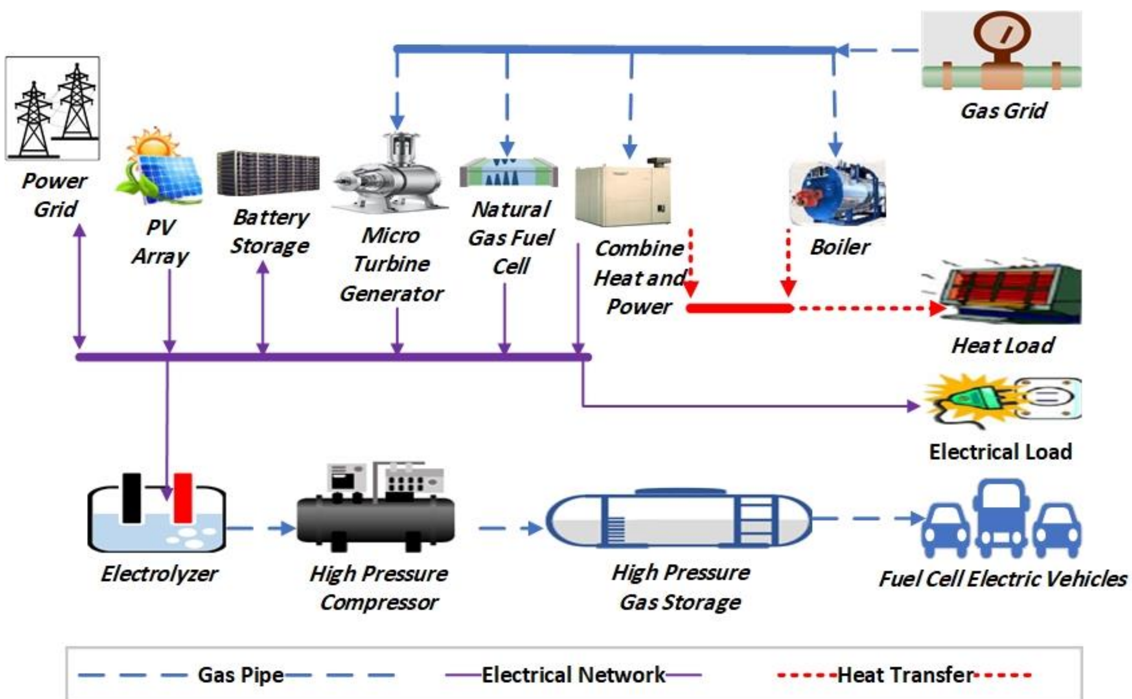

Figure 1: Schematic diagram of the MEMG under study

3 - Mathematical modelling

This section describes the optimal scheduling model for the MG described in Section 2. The whole optimization model is formulated as a Mixed-Integer-Linear Programming problem so that commercial solvers can easily solve it [12].

3.1 - Objective function

The scheduling tool is formulated from the point of view of the MG operator, who presumably aims at operating the grid at minimum cost and, if possible, obtain benefits from selling energy to upscale grids. In this sense, the total operational cost of the MG under study can be calculated by (1).

$$f = \Delta\tau \cdot \sum_t \left\{ \underbrace{\lambda_t^{buy} \cdot p_t^{buy} - \lambda_t^{sell} \cdot p_t^{sell}}_{\substack{Electrical\ energy\ exchanged \\ with\ the\ upscale\ grid}} - \underbrace{\gamma^{FCEV} \cdot \rho^{(700)} \cdot g_t^{FCEV}}_{\substack{Benefits\ from \\ FCEV\ refuelling}} + \right.$$

$$\underbrace{\mu^{Comp} \cdot \rho^{(700)} \cdot g_t^{Comp} + \sum_{i \in \left\{ \substack{P2G,FC,PV, \\ MT,CHP,Boil} \right\}} \left\{ \mu^i \cdot p_t^i \right\}}_{Maintenance\ costs} + \underbrace{\sum_{i \in \{FC,MT,CHP,Boil\}} \left\{ \nu \cdot \upsilon^i \cdot p_t^i \right\}}_{Gas\ purchasing} +$$

$$\left. \underbrace{\sum_{i \in \{FC,P2G,MT,CHP\}} \left\{ \sigma^i \cdot \left(\mathrm{on}_t^i + \mathrm{off}_t^i \right) \right\}}_{Start-up\ and\ Shutdown\ costs} \right\} \tag{1}$$

The first term in (1) reflects the expenditure-income balance of exchanging electricity with the upscale grid. In this sense, it is assumed that the MG can purchase or sell energy from/to the upscale grid under a price per kWh tariff. The second term in (1) is the incomes obtained from FCEVs, which pay a price per kg of hydrogen refuelled. The third term in (1) is the operation and maintenance costs of the different units, which are proportional to the total energy consumed/generated over the time horizon [29]. The fourth term in the objective function stands for the cost of NG purchasing from the main grid, which is used on either FC, MT, boiler or

CHP. Lastly, the fifth term in (1) includes the start-up and shutdown costs of various components.

3.2 - MG balances

The constraint (2) ensures the electrical energetic balance in the MG under study at any time instant, without contemplating non-served energy. Whereas the constraints (3) and (4) are analogue to (2) for the heat and hydrogen subsystems, respectively.

$$p_t^{buy} + p_t^{PV} + p_t^{FC} + p_t^{BS,dch} + p_t^{PV} + p_t^{CHP} + p_t^{MT} = p_t^{LD} + p_t^{BS,ch} + p_t^{sell} + p_t^{P2G} + \frac{g_t^{Comp} \cdot \rho^{(700)} \cdot \varepsilon^{Comp}}{\Delta\tau \cdot \eta^{Comp}};\ \forall t \in T \tag{2}$$

$$LHV \cdot \left(p_t^{CHP} \cdot Z^{CHP} + p_t^{boil}\right) = h_t^{LD};\ \forall t \in T \tag{3}$$

$$\frac{\Delta\tau \cdot p_t^{P2G} \cdot \eta^{P2G}}{LHV} = Z^{(700)} \cdot g_t^{Comp,in};\ \forall t \in T \tag{4}$$

3.3 - Upscale networks modelling

It is realistic to assume that the maximum energy that can be purchased from the upscale electrical grid is limited by either contractual or physical bounds [30], as said in the constraint (5). This idea is also applicable to the gas network, as ensured the constraint (6). Lastly, equation (7) forces the buying and selling processes of the electrical network to be complementary.

$$p_t^i \leq \bar{p}^i;\ \forall t \in T \wedge i \in \{buy, sell\} \tag{5}$$

$$\Delta\tau \cdot LHV \cdot \sum_{i \in \left\{ \substack{FC,MT \\ CHP,Boil} \right\}} \left\{p_t^i\right\} \leq \bar{G}^{grid}; \forall t \in T \tag{6}$$

$$u_t^{buy} + u_t^{sell} \leq 1; \forall t \in T \tag{7}$$

3.4 - Dispatchable units modelling

The dispatchable units (FC, MT, CHP, boiler and P2G, in our case) can be modelled by imposing upper and lower limits in the dispatchable energy [29], as said in the constraint (8). On the other hand, equation (9) links their on/off status with commitment variables while the ramp limits are reflected in (10).

$$u_t^i \cdot \underline{p}^i \leq p_t^i \leq u_t^i \cdot \overline{p}^i; \forall t \in T \wedge i \in \{FC, MT, CHP, P2G, Boil\} \tag{8}$$

$$\mathrm{on}_t^i - \mathrm{off}_t^i = u_t^i - u_{t-1}^i; \forall t \in T \backslash t > 1 \wedge i \in \{FC, MT, CHP, P2G\} \tag{9}$$

$$p_{t-1}^i - R \leq p_t^i \leq p_{t-1}^i + R; \forall t \in T \backslash t > 1 \wedge i \in \{FC, MT, CHP, P2G\} \tag{10}$$

3.5 - PV array modelling

The maximum energy that a PV panel can generate is a function of the ambient temperature and solar irradiation [31], and can be calculated by the expression (11).

$$p_t^{PV} \leq \overline{p}^{PV} \cdot [0.25 \cdot \vartheta_t + 0.03 \cdot \vartheta_t \cdot \theta_t + (1.01 - 1.13 \cdot \eta^{\mathrm{PV}}) \cdot \vartheta_t^2];\ \forall t \in T \tag{11}$$

As noted in [31], the expression (11) cannot be directly applied since the value it yields may be eventually higher than the installed capacity. In real life, this situation is unrealistic since solar inverters typically limit the energy given by PV units to their peak rated power, in order to avoid fast degradation of components. In this sense, constraint (12) is necessary.

$$p_t^{PV} \leq \overline{p}^{PV};\ \forall t \in T \tag{12}$$

3.6 - BS modelling

The maximum power that batteries can exchange with the grid is limited by the installed capacity and the energy-to-power ratio [29], as indicated the constraint (13), while the equation (14) models the state of charge of the bank, which is limited by the installed capacity and the depth-of-discharge settings, as said in (15). Lastly, constraint (16) forces the charging and discharging processes of the BS system to be complementary.

$$p_t^{BS,i} \leq u_t^{BS,i} \cdot \frac{\bar{s}^{BS}}{e2P}; \forall t \in T \wedge i \in \{ch, dch\} \tag{13}$$

$$s_t^{BS} = s_{t-1}^{BS} + \Delta\tau \cdot \left(\eta^{BS,ch} \cdot p_t^{BS,ch} - \frac{p_t^{BS,dch}}{\eta^{BS,dch}}\right); \forall t \in T \backslash t > 1 \tag{14}$$

$$(1 - DOD^{BS}) \cdot \bar{s}^{BS} \leq s_t^{BS} \leq \bar{s}^{BS}; \forall t \in T \tag{15}$$

$$u_t^{BS,ch} + u_t^{BS,dch} \leq 1; \forall t \in T \tag{16}$$

The model (14) is not defined for $t = 1$, thereby, the state of charge of the BS needs to be fixed for this time instant. In this paper, as customary (e.g. see [29]), we assume that the batteries are fully charged at the beginning of the time horizon, as forced constraint (17). To keep the model coherent, this same constraint ensures that the state-of-charge at the beginning of the time horizon is equal to the initial state of charge.

$$s_{t=1}^{BS} = s_{t=end}^{BS} = \bar{s}^{BS} \tag{17}$$

3.7 - P2G modelling

In this paper, the P2G unit comprises an electrolyzer, a compression stage and a hydrogen tank, as the previous stage for FCEV refueling. This subsystem can be modelled in a similar way to the BS system. Firstly, the actual hydrogen flow of the compression and storage stages is limited by rate values, as indicated the equations (18) and (19), respectively.

$$g_t^{Comp,in} \leq \Delta\tau \cdot u_t^{Comp,in} \cdot \bar{q}^{HS}; \forall t \in T \tag{18}$$

$$g_t^{FCEV} \leq \Delta\tau \cdot u_t^{FCEV} \cdot \bar{q}^{HS}; \forall t \in T \tag{19}$$

The gas pressure inside hydrogen tanks must be kept within acceptable limits [32]. In this paper, this condition is modelled by limiting the hydrogen stored at any time instant with functional bounds, as indicated constraint (20).

$$(1 - DOD^{HS}) \cdot \bar{g}^{HS} \leq g_t^{HS} \leq \bar{g}^{HS}; \forall t \in T \tag{20}$$

The expression (21) models the state of charge of the hydrogen vessel, which has to be fixed for the initial and final time instants, similar to the BS. Finally, the complementarity condition (22) completes the P2G model.

$$g_t^{HS} = g_{t-1}^{HS} + g_t^{Comp,in} - g_t^{FCEV}; \forall t \in T \backslash t > 1 \tag{21}$$

$$u_t^{HS,in} + u_t^{HS,out} \leq 1; \forall t \in T \tag{22}$$

Similar to BS, the P2G model requires setting the initial state-of-charge of the hydrogen tank. As in the case of the BS, we assume that the hydrogen vessels are totally filled at the beginning and end of the time horizon, which is ensured by the constraint (23).

$$g_{t=1}^{HS} = g_{t=end}^{HS} = \bar{g}^{HS} \tag{23}$$

4 - Uncertainties modelling

In contrast to most of the related literature in which only one method is considered to model the different uncertain parameters involved, in this paper, we propose to use different approaches depending on the stochastic parameter. We consider this solution more suitable due to each uncertain parameter has its own characteristics. This way, a model which is suitable for this kind of uncertainty may be unsuitable for other ones. Specifically, in this paper, we develop a robust-bi-stochastic optimization framework, by which refueling events and weather uncertainties are modelled via stochastic approaches and demand is managed with IGDT.

4.1 - Stochastic programming for FCEV demand modelling

Refueling patterns of FCEVs are subjected to a strong stochastic behavior. Indeed, both the starting time of the refueling process and the total amount of hydrogen refueled mainly depend on the number of vehicles in a fleet at any time instant and average daily mileage, respectively [33]. In this paper, we consider the stochastic programming developed in [34], to model the uncertain of FCEV demand. This approach consists of modelling the refueling demand by means of Gaussian distributions. Specifically, for refueling starting times this approach considers two time frames 9 AM - 9 PM and 10 PM to 8 AM. For the first time range, scenarios are generated according to a Gaussian distribution with a mean of 6.26 and a standard deviation equal to 1.12. For the second time slot a Gaussian distribution with a mean of 1.7 and standard deviation of 0.9.

For the amount of hydrogen refueled, the range of data is taken from the NREL's archive [35]. This information is thus adjusted to a Gaussian distribution with a mean of 3.45 and a standard deviation of 1.9.

According to the Law of the great numbers, the stochastic character of an uncertain parameter can be effectively represented if a huge amount of scenarios are generated (~1,000 [14]). This amount of information is difficult to tractable in practice. To overcome this issue, we propose to use clustering reduction techniques [36]. More specifically, we have followed the reduction procedure described in [37], by which the scenario space is reduced to the representative scenario set by using the k-medoids technique. Thereby, the amount of scenarios is notably reduced and only the most representative profiles are considered in simulations.

4.2 - Electrical and heat demand modelling via IGDT approach

IGDT is a type of robust optimization that is used in this paper to cope with uncertainties in electrical and heat demand. This approach allows to posing two different strategies for MG operation namely risk-averse and opportunity-seeker [38]. In the former, the MG operator aims at obtaining the proper scheduling plan in a way to be immune against high increases in the objective function, due to the variability of uncertain parameters. In contrast, the opportunity-seeker is an optimistic strategy that assumes favorable values of the uncertainties. In this paper, we assume the MG operator follows a conservative strategy, which aims at minimizing the risk of non-served energy. Given an uncertain parameter ψ, let us assume known its expected value $\hat{\psi}$, then, one could define the so-called radius of uncertainty α, as follows:

$$\phi\left(\hat{\psi}, \alpha\right) = \left\{\alpha : \frac{\psi - \hat{\psi}}{\hat{\psi}} \leq \alpha\right\} \tag{24}$$

where ϕ is a function that describes the behaviour of the random variable. As seen in (24), the radius of uncertainty is a way to define the maximum deviation of the uncertain parameter with respect to its expected value.

For the risk-averse strategy, one needs to determine the base value of the objective function f_b, which is calculated by solving the original problem from a deterministic point of view, i.e. taking the expected values of uncertain parameters. Then, the decision-maker assumes a certain degradation of this objective function because of the action of uncertainties in an unfavorable way. Let us define the assumable increment of the objective function by the pre-set parameter β (in per unit). Therefore, the IGDT based solution with a risk-averse strategy is obtained by solving the following problem.

$$\max_{\boldsymbol{x},\boldsymbol{\Psi},\alpha} f \tag{25}$$

Subject to:

$$f \leq f_b \cdot (1 + \beta) \tag{26}$$

$$\frac{\psi - \hat{\psi}}{\hat{\psi}} \leq \alpha, \forall \psi \in \boldsymbol{\Psi} \tag{27}$$

The remainder constraints of the original problem.

where $\boldsymbol{\Psi}$ is the set of uncertainties.

4.3 - Weather uncertain modelling via the Hong 2m + 1 approach

Point Estimate methods (PEMs) are a family of approximate approaches for the analytical modelling of random variables [39]. In contrast to the classical Monte Carlo method, PEMs are computationally less demanded since it is not necessary to simulate a large number of scenarios [40]. This family of techniques exploits the information provided by the first central moments of the input random variable [41]. In this paper, we use the Hong 2m + 1 method, which is a type of Point Estimate technique because of its overall good properties [42].

In the Hong 2m + 1 method, m stands for the total number of input random variables, therefore, the uncertain set can be represented as:

$$\phi(\mathbf{\Psi}) = \phi(\psi_1, \psi_2, \dots, \psi_d, \dots, \psi_m) \tag{28}$$

The considered Hong method converts the original problem with m input random variables, into 2m + 1 equivalent deterministic problems. For each input variable, the Hong's method considers three concentration points instead of the probability density function. Thus, each input variable comprises three different locations fully described by the p^{th} location ($\psi_{d,p}$) and weighting factor ($\omega_{\psi_{d,p}}$). Considering that each variable is defined by its mean (μ_{ψ_d}) and standard deviation (σ_{ψ_d}), the following set of equations are focused on calculating the locations and weighting factors of each input variable.

$$\psi_{d,p} = \mu_{\psi_d} + \xi_{\psi_{d,p}} \cdot \sigma_{\psi_d};\ \forall d \in \{1,2,\dots,m\} \wedge p \in \{1,2,3\} \tag{29}$$

where $\xi_{\psi_{d,p}}$ is calculated for each input variable as follows:

$$\xi_{\psi_{d,p}} = \frac{\lambda_{\psi_{d,3}}}{2} + (-1)^{3-p} \cdot \sqrt{\lambda_{\psi_{d,4}} - \frac{3}{4} \cdot \lambda_{\psi_{d,3}}^2}; \forall d \in \{1,2,\dots,m\} \wedge\ p \in \{1,2\} \tag{30}$$

$$\xi_{\psi_{d,3}} = 0;\ \forall d \in \{1,2,\dots,m\} \tag{31}$$

$$\lambda_{\psi_{d,3}} = \frac{E\left[\left(\psi_d - \mu_{\psi_d}\right)^3\right]}{\sigma_{\psi_d}^3}, \lambda_{\psi_{d,4}} = \frac{E\left[\left(\psi_d - \mu_{\psi_d}\right)^4\right]}{\sigma_{\psi_d}^4}; \forall d \in \{1,2,\dots,m\} \tag{32}$$

where $E[*]$ yields the expected value of an input random variable; and $\lambda_{\psi_{d,3}}$ and $\lambda_{\psi_{d,4}}$ are respectively the skewness and the kurtosis of the d^{th} random variable (see [41]). Finally, the weighting factors are calculated by (33) and (34).

$$\omega_{\psi_{d},p} = \frac{(-1)^{3-p}}{\xi_{\psi_{d,p}} \cdot \left(\xi_{\psi_{d,1}} - \xi_{\psi_{d,2}}\right)}; \forall d \in \{1,2,\dots,m\} \wedge\ p \in \{1,2\} \tag{33}$$

$$\omega_{\psi_{d,3}} = \frac{1}{m} - \frac{1}{\lambda_{\psi_{d,4}} - \lambda_{\psi_{d,3}}^2}; \forall d \in \{1,2,\dots,m\} \tag{34}$$

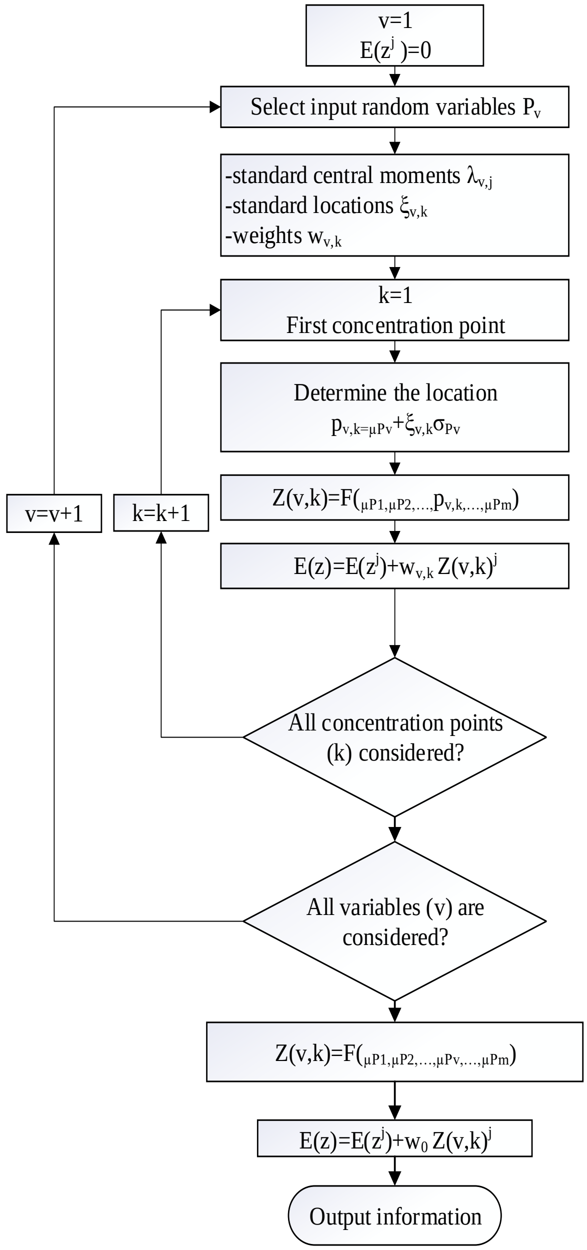

Figure 1: 2m+1 Hong approach

In this paper, irradiation level and ambient temperature is considered as uncertain variables and the PV output which is function of these parameters is modeled via Hong method.

5 - Case study

This section presents various numerical results on a benchmark MEMG as described in section 2, with the aim of validating the scheduling tool developed in this paper. The results have been obtained by running the optimal scheduling tool developed in Section 3 over a 24 hours time horizon with 15 minutes time resolution. The different uncertainties have been modelled by using different approaches, as described in Section 4. Thus, the FCEV demand has been modelled by stochastic programming, the uncertainty on weather parameters has been treated with the Hong 2m + 1 technique while the electrical and heat demands have been managed with the IGDT approach.

All simulations were performed on an Intel® corei7 CPU with 8GB RAM. The Mixed-Integer-Linear programming model described in Section 3 was coded in Matlab R2019a and solved using Gurobi [43]. Preliminary experiments performed by the authors took 10-20 minutes on average, which can be considered acceptable for day-ahead tools which may have various hours to be executed.

5.1 - Input data

Tables 1-7 provide the input data necessary for simulations. The different equipment parameters have been extracted from different references [45-50]. On the other hand, Fig. 3-6 plots the expected values for the heat and electrical demands, ambient temperature and solar irradiation, respectively. These expected values correspond to real observed profiles that can be found in [50-52].

Table1: power generation/usage limits

Parameter	Value
$\overline{p}^{buy}/\overline{p}^{sell}$	50/400 kW
$\underline{p}^{p2g}/\overline{p}^{p2g}$	10/100 kW
$\underline{p}^{FC}/\overline{p}^{FC}$	15/50 kW
$\underline{p}^{CHP}/\overline{p}^{CHP}$	0/100 kW
$\underline{p}^{MT}/\overline{p}^{MT}$	0/15 kW
$\underline{p}^{Boil}/\overline{p}^{Boil}$	0/120 kW

Table2: hydrogen tank data

Parameter	Value
$\bar{g}^{HS}$	500 kg
$\underline{g}^{HS}$	300 kg
$\bar{q}^{HS}$	120 m³/h
$g_{t=1}^{HS}$	120 m³/h

Table3: hydrogen compressor data

Parameter	Value
$\overline{g}^{comp,in}/\overline{g}^{comp,out}$	120/120 m³/h
ε^{Comp}	2.7 kWh/m³
$Z^{(700)}$	1.4
$\rho^{(700)}$	40 kg/m³
ε^{Comp}	2.7 kWh/m³
LHV	39.8 kWh
$\eta^{(700)}$	0.7
$\mu^{(700)}$	0.11 $/kg
γ	7 $/kg

Table4: data of battery storage system

Parameter	Value
$\overline{p}^{BS,ch}$	15 kW
$\overline{p}^{BS,dch}$	15 kW
$\bar{s}^{BS}$	100 kWh
$s_{t=1}^{BS}$	100 kWh

Table 5: CHP, FC, MT and P2G data

Parameter	**Value**
Z^{CHP}	1.2
R^{FC}	15 kW
μ^{p2g}/μ^{FC}	0.01/0.04 \$/kWh
$\sigma^{FC}/\sigma^{CHP}/\sigma^{MT}/\sigma^{p2G}$	0.42/0.31/0.64/0.22 \$

Table6: Equipment efficiencies

Parameter	***Value***
η^{P2G}	0.7
η^{FC}	0.7
η^{BS}	0.9
η^{MT}	0.75

Table7: NG nominal consumption of generators

Parameter	**Value**
υ^{Boil}	0.073 m^3/kWh
υ^{FC}	0.079 m^3/kWh
υ^{MT}	0.042 m^3/kWh
υ^{CHP}	0.098 m^3/kWh
ν	4.77 \$/kg

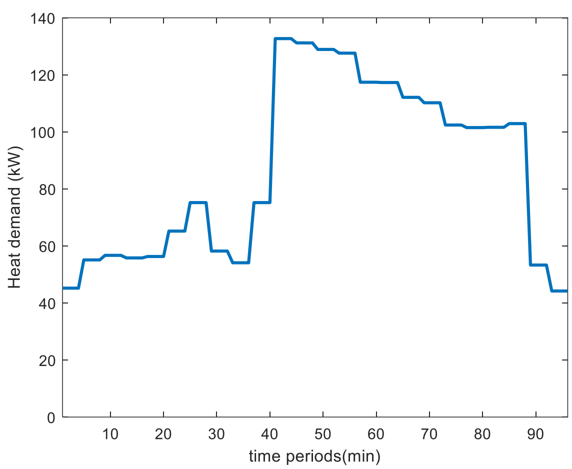

Figure 3: Expected heat demand

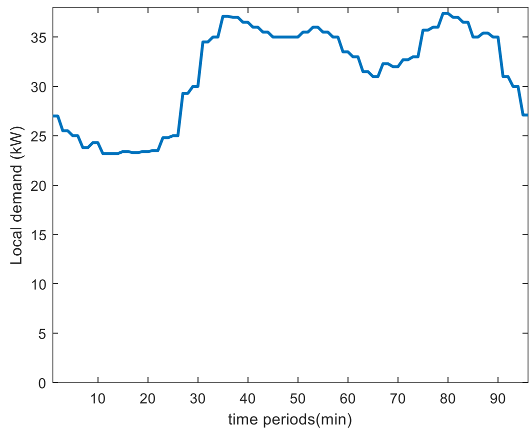

Figure 4: Expected electrical demand

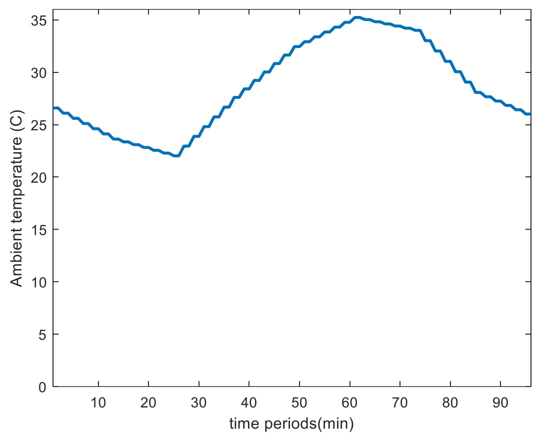

Figure 5: Expected ambient temperature

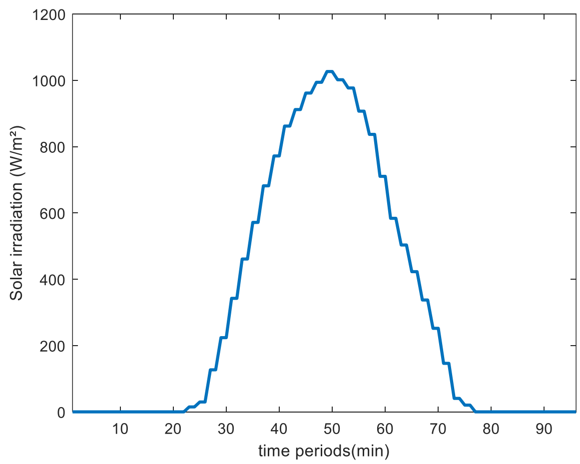

Figure 6: Expected solar irradiation

5.2 - Hong 2m + 1 validation

In this section, the proposed Hong 2m + 1 approach to model the uncertainty in weather parameters is validated by comparison with the well-known Monte Carlo (MC) method [53], which has been considered the benchmark method for stochastic modelling of uncertainties. In this regard, 10000 scenarios with 7% standard deviation have been generated using the Monte Carlo technique and they have been compared with the proposed approach. Fig. 7 compares the results obtained with both concerned approaches. As observed, profiles generated with both approaches were practically the same, which demonstrates the accurateness and effectiveness of the proposed method.

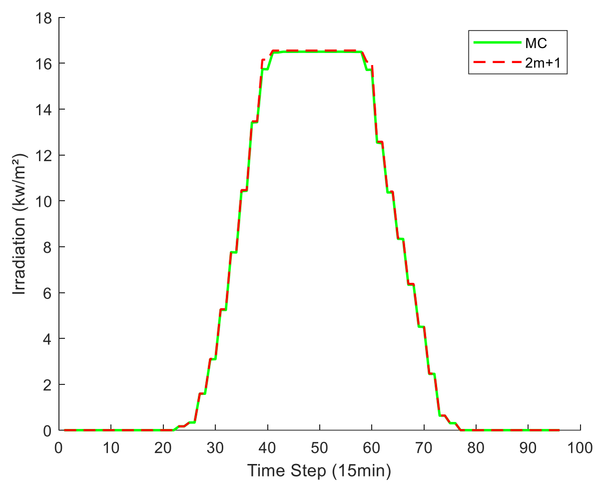

Fig 7: Modelled solar irradiation with MC and Hong 2m + 1

To get a better overview, Fig. 8 and 9 show the real mean square error (RMSE) and absolute error for different standard deviations. As expected, both indicators grow with the standard deviation, however, notable differences are only achieved with very high values of standard deviations. Even so, the possible errors introduced by the Hong 2m + 1 simplification are really marginal and inappreciable in simulations.

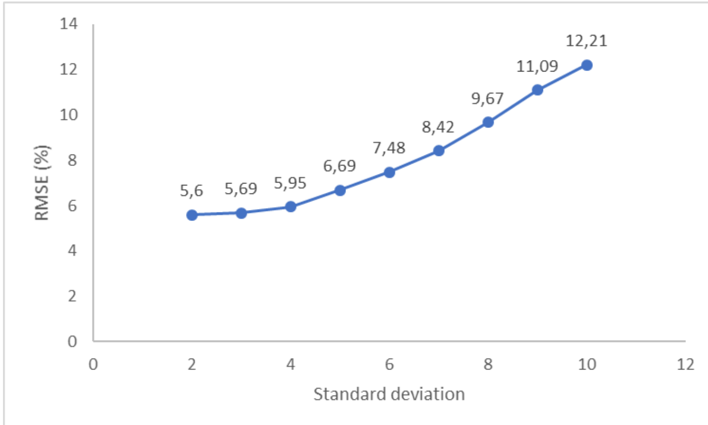

Figure 8: RMSE of the Hong 2m + 1 approach in comparison with MC

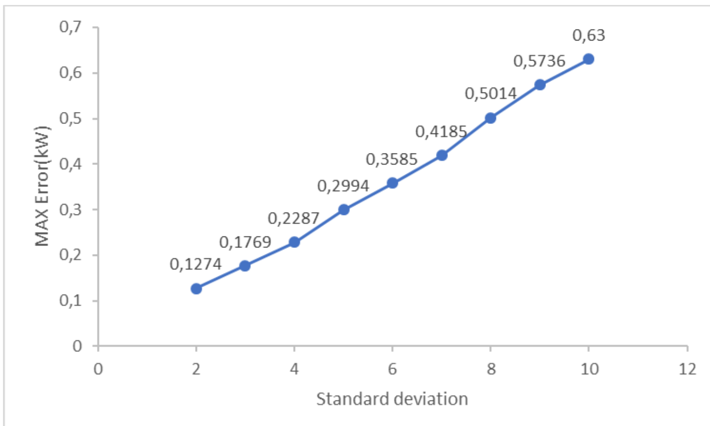

Figure 9: maximum absolute error introduced by Hong 2m + 1 compared with MC

5.3 - Results

The studied MEMG was simulated considering the uncertain profiles described in previously described methods. Figure 10 compare results of optimization for the total cost of MEMG using different uncertainty modelling.

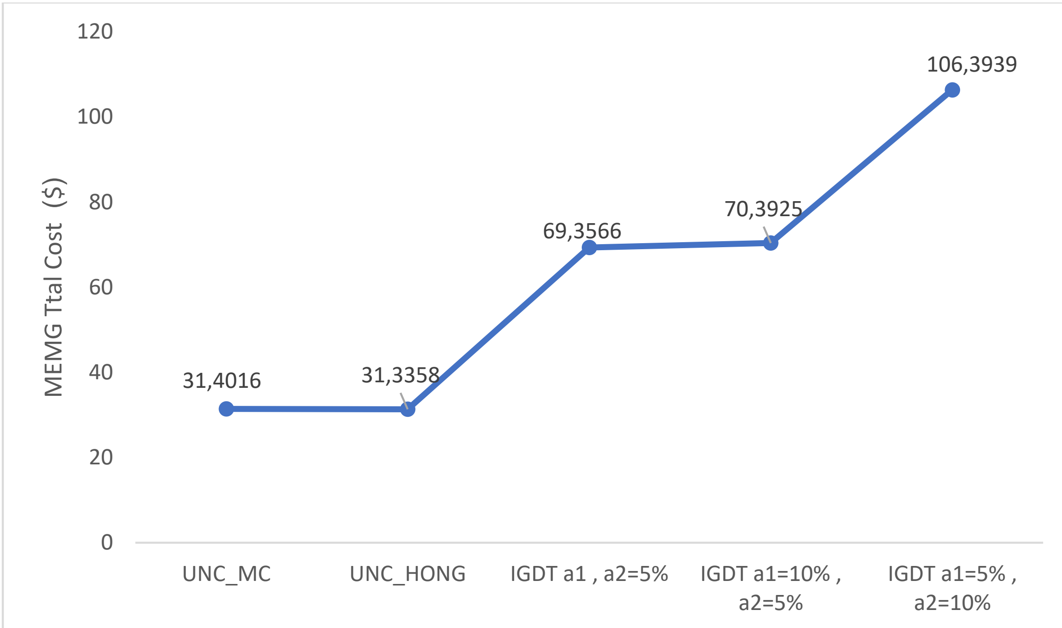

Figure 10: Comparative cost of MEMG considering various uncertainty modeling

As seen, considering just ambient temperature and solar irradiation uncertainty with 10% standard deviation, the total cost of the MEMG via MC uncertainty approach is $31.4016 while it is $31.3358 for Hong's 2m+1 approach. The difference in the objective function with both methods only differs by ~0.2%, which strengthens the idea that the developed model is accurate and effective. It is obvious that for a higher standard deviation or lower number of MCS scenarios, this difference can be increased.

When considering the uncertainty of electrical and heat loads in addition to PV output uncertainty with the IGDT approach in different radius of uncertainty ($\alpha 1$ and $\alpha 2$), the total cost is significantly increased. As figure 10 shows, the radius of uncertainty in heat loads has more effect on the total cost in our case study. In the following, the optimal operation of MEMG is done considering a radius of 5% for the IGDT approach of both electrical and heat load, and a standard deviation of 10% for MCS.

Fig. 11 plots the scheduling plan for the electrical grid (buying-selling energy). As seen, the studied system mostly sells energy during the evening, which is propitiated by a high PV potential along with large fuel cell and MT generation, as seen in Fig. 12. In this case, gas purchasing is more economic than electricity cost, in such a situation, the scheduling tool determines economically attractive producing electrical energy from gas-to-power units to be sold to the grid, taking advantage of high energy pricing during these periods.

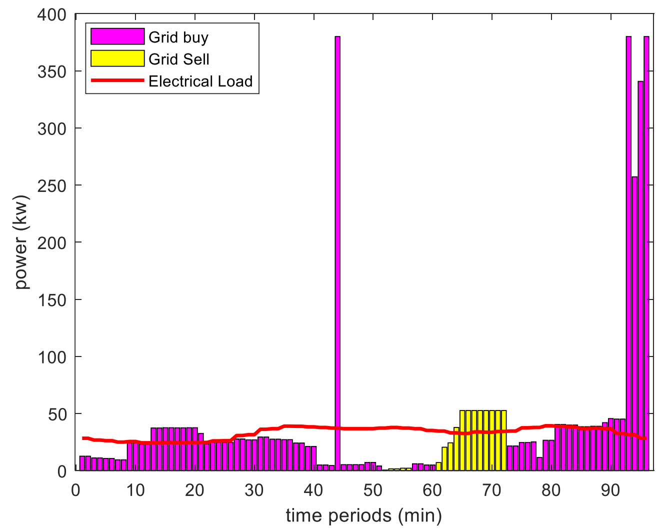

Figure 11: Scheduling result for the electrical upscale network

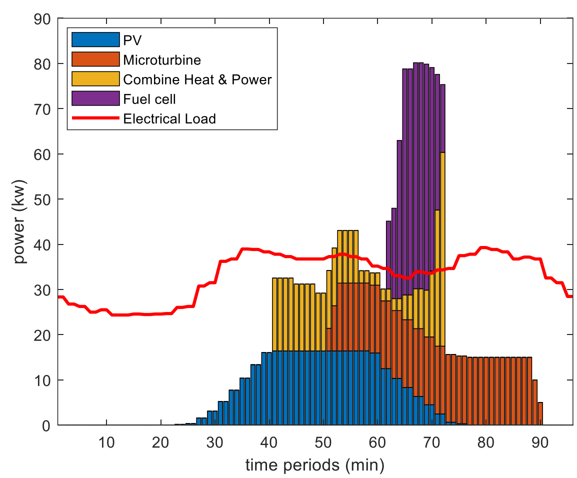

Figure 12: Generation scheduling result for the case study

Figure 13 shows the scheduling plan for the FC and P2G unit. As observed, P2G is scheduled to produce hydrogen which is entirely dedicated to cover the FCEV refuelling demand, from which the MG operator obtains high benefits. On the other hand, the FC is mostly operated during the evening. As seen, this operation procedure aims at obtaining benefits of high energy pricing. Thereby, the electricity produced through fuel cells is entirely sold to the grid, as saw in Fig. 12.

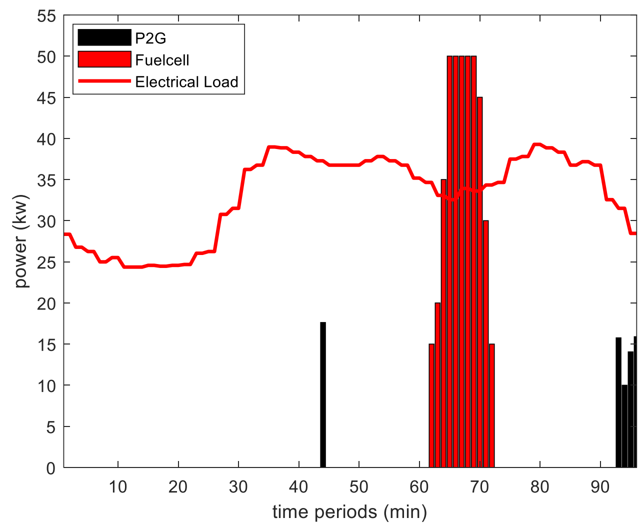

Figure 13: Scheduling result for the FC and the P2G system

As seen in Fig. 13, the P2G unit is operated during two well-distinguished time periods. The first one occurs at midday, during which the P2G unit refills the hydrogen tank, which is partially emptied due to high FCEV demand. On the other hand, the P2G tends to be deeply operated during the night. This is because the hydrogen tank needs to be refilled as seen in Fig. 14. This operation is more attractive during the night, when the energy price is falling down.

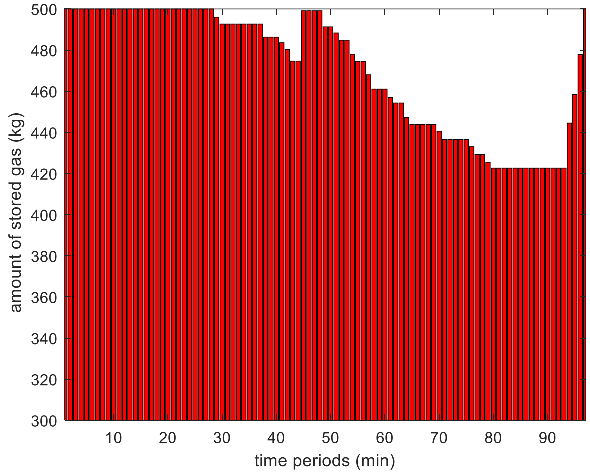

Figure 14: State-of-charge of the hydrogen tank

As seen in Fig. 15, scheduling plan for the BS system presents two clear charging periods. One of them occurs during dawn and the other during night. The first one tries to fully charge the battery system, exploiting the lowest energy price during dawn. The second one aims at fully recovering the state-of-charge of the batteries, taking advantage of low energy pricing during night.

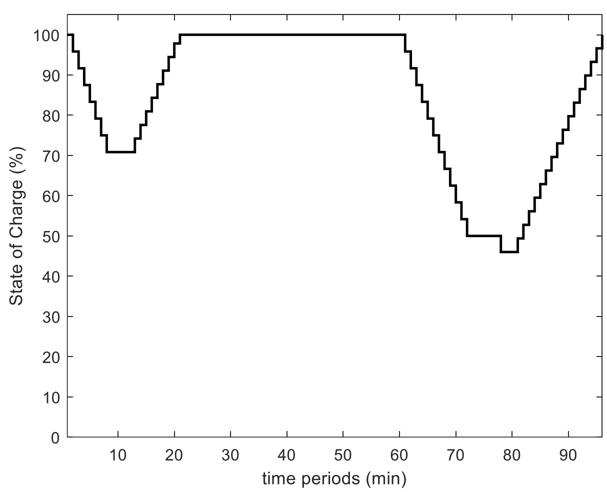

Figure 15: State-of-charge of the battery system

Lastly, we focus on the heat subsystem. In this regard, Fig. 16 and 17 plots the scheduling plan for the boiler and CHP, respectively. As seen, most of heat demand is covered by the boiler. Its operation is more economical than the CHP which is also mostly devoted on producing electricity from natural gas, as observed in Fig. 12. Nevertheless, the CHP unit partially covers the heat demand during midday-evening. During midday, the boiler hits its upper bound and the surplus heat demand needs to be supplied from the CHP, while during the evening, high PV potential allows to exploit the CHP for producing heat instead of electricity.

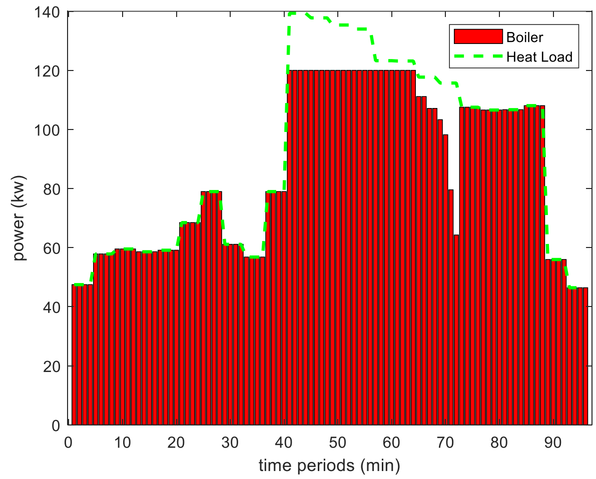

Figure 16: Scheduling result for the boiler

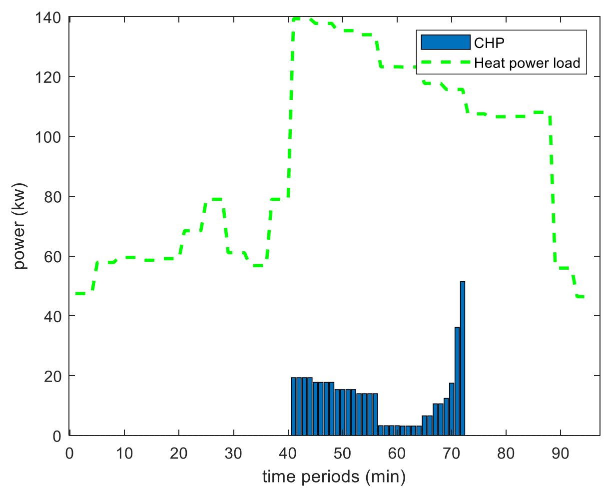

Figure 17: Scheduling result for the CHP

6 - conclusion

In this paper, a bi-stochastic-robust framework for the optimal operation of a MEMG has been proposed. The proposed model poses an optimal scheduling tool for a MEMG which encompasses electric, thermal, gas and hydrogen subsystems. The uncertainties are treated by using different approaches according to the characteristics of each stochastic parameter. Thereby, the IGDT is used to model electrical and heat demand and the Hong 2m+1 is applied to handle the uncertainty of the PV system. Furthermore, a stochastic approach is used to deal with the accidental behavior of FCEVs.

To validate the developed model, extensive simulation was performed on a MEMG test system consisting of renewable and non-renewable resources, different storage systems and P2G technology. The results showed the effectiveness of the developed model, which is able with manage different uncertainties with strong different natures in an efficient way. The results reported were coherent and respond to the normal operation of this kind of system under uncertainty, which confirms the effectiveness of the model.

Future works should be focused on applying the proposed bi-stochastic-robust framework to other related problems like MG expansion planning.

References

[1] E. Hossain, E. Kabalci, R. Bayindir, R. Perez. Microgrid testbeds around the world: State of art. *Energy Conversion & Management* 2014; 86: 132-53. 10.1016/j.enconman.2014.05.012.

[2] R. K. Chauhan, K. Chauhan. *Distributed Energy Resources in Microgrids: Integration, Challenges and Optimization*. Academic Press, Cambridge, MA; 2019. 10.1016/C2018-0-02714-0.

[3] F. Bandeiras, E. Pinheiro, M. Gomes, P. Coelho, J. Fernandes. Review of the cooperation and operation of microgrid clusters. *Renewable & Sustainable Energy Reviews* 2020; 133: 110311. 10.1016/j.rser.2020.110311.

[4] M. F. Zia, E. Elbouchikhi, M. Benbouzid. Microgrids energy management systems: A critical review on methods, solutions, and prospects. *Applied Energy* 2018; 222: 1033-55. 10.1016/j.apenergy.2018.04.103.

[5] S. Tan, et al. New Challenges in the Design of Microgrid Systems: Communication Networks, Cyberattacks, and Resilience. *IEEE Electrification Magazine* 2020; 8(4): 98-106. 10.1109/MELE.2020.3026496.

[6] D. Xu, Q. Wu, B. Zhou, C. Li, L. Bai, S. Huang. Distributed Multi-Energy Operation of Coupled Electricity, Heating, and Natural Gas Networks. *IEEE Transactions on*

Sustainable Energy 2020; 11(4): 2457-2469. https://doi.org/10.1109/TSTE.2019.2961432.
[7] J. He, Z. Yuan, X. Yang, W. Huang, Y. Tu, Y. Li. Reliability Modeling and Evaluation of Urban Multi-Energy Systems: A Review of the State of the Art and Future Challenges. *IEEE Access* 2020; 8: 98887-98909https://doi.org/10.1109/ACCESS.2020.2996708.
[8] M. Tostado-Véliz, P. Arévalo, F. Jurado. A Comprehensive Electrical-Gas-Hydrogen Microgrid Model for Energy Management Applications. *Energy Conversion & Management* 2021; 228: 113726. 10.1016/j.enconman.2020.113726.
[9] Q. Wang, J. Liu, Y. Hu, X. Zhang. Optimal Operation Strategy of Multi-Energy Complementary Distributed CCHP System and its Application on Commercial Building. *IEEE Access* 2019; 7: 127839-127849. https://doi.org/10.1109/ACCESS.2019.2939913.
[10] A. L. Bukar, C. W. Tan, L. K. Yiew, R. Ayop, W. S. Tan. A rule-based energy management scheme for long-term optimal capacity planning of grid-independent microgrid optimized by multi-objective grasshopper optimization algorithm. *Energy Conversion & Management* 2020; 221: 113161. 10.1016/j.enconman.2020.113161.
[11] M. K. Kiptoo, et al. Integrated approach for optimal techno-economic planning for high renewable energy-based isolated microgrid considering cost of energy storage and demand response strategies. *Energy Conversion & Management* 2020; 215: 112917. 10.1016/j.enconman.2020.112917.
[12] N. G. Paterakis, O. Erdinç, A. G. Bakirtzis, J. P. S. Catalão. Optimal Household Appliances Scheduling Under Day-Ahead Pricing and Load-Shaping Demand Response Strategies. *IEEE Transactions on Industrial Informatics* 2015; 11(6): 1509-19. 10.1109/TII.2015.2438534.
[13] N. Good, P. Mancarella. Flexibility in Multi-Energy Communities With Electrical and Thermal Storage: A Stochastic, Robust Approach for Multi-Service Demand Response. *IEEE Transactions on Smart Grid* 2019; 10(1): 503-513. https://doi.org/10.1109/TSG.2017.2745559.
[14] H. Rashidizadeh-Kermani, M. Vahedipour-Dahraie, A. Anvari-Moghaddam, J. M. Guerrero. A stochastic bi-level decision-making framework for a load- serving entity in day-ahead and balancing markets. *International Transactions on Electrical Energy Systems* 2019; 29(11): e12109. https://doi.org/10.1002/2050-7038.12109.
[15] G. Cau, D. Cocco, M. Petrollese, S. Knudsen Kær, C. Milan. Energy management strategy based on short-term generation scheduling for a renewable microgrid using a hydrogen storage system. *Energy Conversion & Management* 2014; 87: 820-31. https://doi.org/10.1016/j.enconman.2014.07.078.
[16] M. Tostado-Véliz, R. S. León-Japa, F. Jurado. Optimal electrification of off-grid smart homes considering flexible demand and vehicle-to-home capabilities. *Applied Energy* 2021; 298: 117184. https://doi.org/10.1016/j.apenergy.2021.117184.
[17] M. Petrollese, L. Valverde, D. Cocco, G. Cau, J. Guerra. Real-time integration of optimal generation scheduling with MPC for the energy management of a renewable hydrogen-based microgrid. *Applied Energy* 2016; 166: 96-106. https://doi.org/10.1016/j.apenergy.2016.01.014.
[18] S. A. Kostantinopoulos, A. G. Anastasiadis, G. A. Vokas, G. P. Kondylis, A. Polyzakis. Optimal management of hydrogen storage in stochastic smart microgrid

operation. *International Journal of Hydrogen Energy* 2018; 43(1): 490-9. https://doi.org/10.1016/j.ijhydene.2017.06.116.
[19] S. Nojavan, A. Akbari-Dibavar, A. Farahmand-Zahed, K. Zare. Risk-constrained scheduling of a CHP-based microgrid including hydrogen energy storage using robust optimization approach. *International Journal of Hydrogen Energy* 2020; 45(56): 32269-84. https://doi.org/10.1016/j.ijhydene.2020.08.227.
[20] T. Sriyakul, K. Jermsittiparsert. Risk-constrained design of autonomous hybrid refueling station for hydrogen and electric vehicles using information gap decision theory. *International Journal of Hydrogen Energy* 2021; 46(2): 1682-93. https://doi.org/10.1016/j.ijhydene.2020.10.137.
[21] B. Li, R. Roche, A. Miraoui. Microgrid sizing with combined evolutionary algorithm and MILP unit commitment. *Applied Energy* 2017; 188: 547-62. https://doi.org/10.1016/j.apenergy.2016.12.038.
[22] F. Alavi, E. P. Lee, N. van de Wouw, B. De Schutter, Z. Lukszo. Fuel cell cars in a microgrid for synergies between hydrogen and electricity networks. *Applied Energy* 2017; 192: 296-304. https://doi.org/10.1016/j.apenergy.2016.10.084.
[23] W. Liu, C. Liu, Y. Lin, K. Bai and L. Ma. Interval Multi-Objective Optimal Scheduling for Redundant Residential Microgrid With VESS. *IEEE Access* 2019; 7: 87849-65. https://doi.org/10.1109/ACCESS.2019.2923612.
[24] H. Khaloie, A. Anvari-Moghaddam, J. Contreras, P.Siano. Risk-involved optimal operating strategy of a hybrid power generation company: A mixed interval-CVaR model. *Energy* 2021; 232: 120975. https://doi.org/10.1016/j.energy.2021.120975.
[25] Seok-Ho Seo, Si-Doek Oh, Jinwon Park, Hwanyeong Oh, Yoon-Young Choi, Won-Yong Lee, Ho-Young Kwak. Thermodynamic, exergetic, and thermoeconomic analyses of a 1-kW proton exchange membrane fuel cell system fueled by natural gas, Energy, Volume 217, 2021.
[26] P. Kalra, R. K. Garg, A. Kumar. Parametric sensitivity analysis for a natural gas fueled high temperature tubular solid oxide fuel cell. *Heliyon* 2020; 6(7): e04450. https://doi.org/10.1016/j.heliyon.2020.e04450.
[27] G. Muriithi, S. Chowdhury. Optimal Energy Management of a Grid-Tied Solar PV-Battery Microgrid: A Reinforcement Learning Approach. *Energies* 2021; 14: 2700. https://doi.org/10.3390/en14092700.
[28] J. Kurtz, S. Sprik, G. Saur and S. Onorato. Fuel Cell Electric Vehicle Driving and Fueling Behavior. *National Renewable Energy Laboratory* 2019; Denver, CO, U.S., Rep. no. NREL/TP-5400-73010. Available at: https://www.nrel.gov/docs/fy19osti/73010.pdf (Accessed June 7, 2021).
[29] P. Arévalo, M. Tostado-Véliz, F. Jurado. A Novel Methodology for Comprehensive Planning of Battery Storage Systems. *Journal of Energy Storage* 2021; 37: 102456. https://doi.org/10.1016/j.est.2021.102456.
[30] M. Tostado-Véliz, S. Mouassa, F. Jurado. A MILP Framework for Electricity Tariff-choosing Decision Process in Smart Homes Considering 'Happy Hours' Tariffs. *International Journal of Electrical Power & Energy Systems* 2021; 131: 107139. https://doi.org/10.1016/j.ijepes.2021.107139.
[31] M. Tostado-Véliz, M. Bayat, A. A. Ghadimi, F. Jurado. Home Energy Management in off-grid Dwellings: Exploiting Flexibility of Thermostatically Controlled

Appliances. *Journal of Cleaner Production* 2021; 310: 127507. https://doi.org/10.1016/j.jclepro.2021.127507.

[32] J. Jannati, D. Nazarpour. Optimal energy management of the smart parking lot under demand response program in the presence of the electrolyser and fuel cell as hydrogen storage system. *Energy Conversion & Management* 2017; 138: 659-69. https://doi.org/10.1016/j.enconman.2017.02.030.

[33] S. Negarestani, M. Fotuhi-Firuzabad, M. Rastegar, A. Rajabi-Ghahnavieh. Optimal Sizing of Storage System in a Fast Charging Station for Plug-in Hybrid Electric Vehicles. *IEEE Transactions on Transportation Electrification* 2016; 2(4): 443-53. https://doi.org/10.1109/TTE.2016.2559165.

[34] U. Mukherjee, A. Maroufmashat, A. Narayan, A. Elkamel, M. Fowler. A Stochastic Programming Approach for the Planning and Operation of a Power to Gas Energy Hub with Multiple Energy Recovery Pathways. *Energies* 2017; 10(7): 868. https://doi.org/10.3390/en10070868.

[35] J. Kurtz, S. Sprik, G. Saur, S. Onorato. Fuel Cell Electric Vehicle Driving and Fueling Behavior. *National Renewable Energy Laboratory*, 2019, NREL/TP-5400-73010. Online available at: https://www.nrel.gov/docs/fy19osti/73010.pdf, (accessed Jun. 30, 2021).

[36] E. S. Pinto, L. M. Serra, A. Lázaro. Evaluation of methods to select representative days for the optimization of polygeneration systems. *Renewable Energy* 2020; 151: 488-502. https://doi.org/10.1016/j.renene.2019.11.048.

[37] M. Tostado-Véliz, D. Icaza-Alvarez, F. Jurado. A Novel Methodology for Optimal Sizing Photovoltaic-Battery Systems in Smart Homes considering Grid Outages and Demand Response. *Renewable Energy* 2021; 170: 884-96. https://doi.org/10.1016/j.renene.2021.02.006.

[38] A. Dolatabadi, M. Jadidbonab, B. Mohammadi-Ivatloo. Short-Term Scheduling Strategy for Wind-Based Energy Hub: A Hybrid Stochastic/IGDT Approach. *IEEE Transactions on Sustainable Energy* 2019; 10(1): 438-48. https://doi.org/10.1109/TSTE.2017.2788086.

[39] S. Ghaemi, F. Hamzeh Aghdam, A. Safari, M. Farrokhifar. Stochastic economic analysis of FACTS devices on contingent transmission networks using hybrid biogeography-based optimization. *Electrical Engineering* 2019; 101(3): 829-43. https://doi.org/10.1007/s00202-019-00825-6.

[40] B. Faridpak, A. Alahyari, M. Farrokhifar, H. Momeni. Toward Small Scale Renewable Energy Hub-Based Hybrid Fuel Stations: Appraising Structure and Scheduling. *IEEE Transactions on Transportation Electrification* 2020; 6(1): 267-77. https://doi.org/10.1109/TTE.2020.2972382.

[41] H. R. Massrur, T. Niknam, M. Fotuhi-Firuzabad. Investigation of carrier demand response uncertainty on energy flow of renewable-based integrated electricity-gas-heat systems. *IEEE Transactions on Industrial Informatics* 2018; 14(11): 5133-42. https://doi.org/10.1109/TII.2018.2798820.

[42] J. M. Morales, J. Perez-Ruiz. Point estimate schemes to solve the probabilistic power flow. *IEEE Transactions on Power Systems* 2007; 22(4): 1594-01. https://doi.org/10.1109/TPWRS.2007.907515.

[43] Gurobi - the fastest solver. www.gurobi.com (Accessed July 7, 2021)

[44] U. Mukherjee, A. Maroufmashat, A. Narayan, A. Elkamel and M. Fowler, "A Stochastic Programming Approach for the Planning and Operation of a Power to Gas Energy Hub with Multiple Energy Recovery Pathways," *Energies* 2017, 10(7): 868. https://doi.org/10.3390/en10070868

[45] M. Götz, et. al. Renewable Power-to-Gas: A technological and economic review. *Renewable Energy* 2016; 85: 1371-1390. https://doi.org/10.1016/j.renene.2015.07.066.

[46] M. Hirscher, Ed. Handbook of hydrogen storage: new materials for future energy storage. Weinheim, Germany: Wiley-VCH Verlag GmbH & Co. KgaA, 2010.

[47] Z. Salameh, "Energy Storage," in Renewable Energy System Design, Z. Salameh, Ed., Waltham, MA, USA: Academic Press, 2014, ch. 4, pp. 201-298, doi: 10.1016/C2009-0-20257-1

[48] Y. Jiang and L. Guo. Research on Wind Power Accommodation for an Electricity-Heat-Gas Integrated Microgrid System With Power-to-Gas. *IEEE Access* 2019; 7: 87118-87126, 2019. https://doi.org/10.1109/ACCESS.2019.2924577.

[49] G. Parks, R. Boyd, J. Cornish and R. Remick. Hydrogen Station Compression, Storage, and Dispensing Technical Status and Costs. *National Renewable Energy Laboratory*, NREL/BK-6A10-58564, 2014. Accessed: 30 Sept. 2020. Online available at: https://www.nrel.gov/docs/fy14osti/58564.pdf , (Accessed July 7, 2021)

[50] Z. Liu, Q. Wu, M. Shahidehpour, C. Li, S. Huang, and W. Wei, "Transactive Real-time Electric Vehicle Charging Management for Commercial Buildings with PV On-site Generation," IEEE Transactions on Smart Grid, 2018.

[51] National Centers for Environmental Information. Land-Based Datasets and Products. Online available at: https://www.ncdc.noaa.gov/data-access/land-based-stationdata/land-based-datasets, (accessed June 28, 2021).

[52] Red Eléctrica de España. Canary electricity demand in real-time. Online available at: https://www.ree.es/en/activities/canary-islands-electricity-system/canary-electricitydemand- in-real-time, (accessed June 28, 2021).

[53] A. A. Ghadimi, et al. Stochastic transmission expansion planning in the presence of wind farms considering reliability and N-1 contingency using grey wolf optimization technique. *Electrical Engineering* 2021. https://doi.org/10.1007/s00202-021-01339-w